

# AN EFFECTIVE HUMAN IRIS CODE WITH LOW COMPLEXITY

*D. M. Monro and D. Zhang*

Department of Electronic and Electrical Engineering, University of Bath, BA2 7AU, UK  
<http://dmsun4.bath.ac.uk> {d.m.monro, d.zhang} @bath.ac.uk

## ABSTRACT

A human iris coding technique is reported based upon differences in the power spectrum of fragments from normalized iris images. The procedure has been applied to a set of 2174 images from 308 eyes and tuned over a range of parameters. For identity recognition, 100% correct recognition is achieved using a weighted Hamming Distance metric. For identity verification, a variable threshold is applied to the distance metric and the False Acceptance and False Rejection Rates are recorded. After tuning the various parameters, the method achieves the lowest False Acceptance Rate at the point of first False Rejection amongst the three algorithms tested, as well as the lowest complexity.

## 1. INTRODUCTION

Automated personal identification based on biometrics has received considerable attention with increasing emphasis on access control [1]. Among biometric technologies, iris recognition is noted for its high reliability and is currently a subject of great interest in academia and industry [1, 2].

Much work has been done on coding the human iris [3-7]. Daugman [4] filters iris image with a family of multiscale Gabor filters and their phase structure is demodulated into a sequence of complex-valued phasors. These phasors are then projected onto a four quadrant complex plane and a binary iris code is generated from these phasors. Tan [6] generates a bank of 1D intensity signals from the iris image and filters these 1D signals with a special class of wavelet. The positions of local sharp variations are recorded as the features. Both methods have achieved good results.

Two major problems in this field still persist. What is the information in the iris texture that distinguishes one class from others? How can the coding and matching complexity be reduced for practical applications? This paper contributes towards a more realizable solution to these problems.

## 2. IRIS IMAGE NORMALIZATION

An image of the eye, as shown in Figure 1(a), contains information which is not of interest for iris recognition in the pupil, sclera and eyelid. In addition the illumination is not uniform over different images. Thus, prior to coding, the image needs to be pre-processed to eliminate these factors. Figure 1 illustrates the three main pre-processing steps. First, the inner and outer iris boundaries are located to eliminate the pupil and eyelid etc. Then the iris image is transformed from polar co-ordinates to a 512x80 fixed size rectangular image to reduce the effect of iris dilation and contraction, of which 512x48 will be coded. The non-uniform background illumination is finally homogenized.

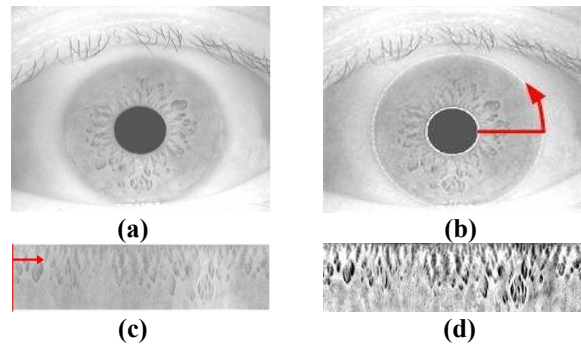


**Figure 1.** Iris Image Pre-Processing  
(a) Original Image (b) Localized Image  
(c) Unwrapped Image (d) Enhanced Image

## 3. PROPOSED IRIS CODING TECHNIQUE

The image of a human iris is highly specific to the individual, whose two eyes are also unique. In order to represent this information, Daugman [4] uses local phase variation and Tan [6] captures local intensity variation. In this paper, we will exploit the local frequency variation as another novel method for coding the iris image.

### 3.1 Segmentation into Patches

Figure 2 shows how we divide the iris image into rectangular patches with particular size and orientation to apply the proposed iris coding technique.

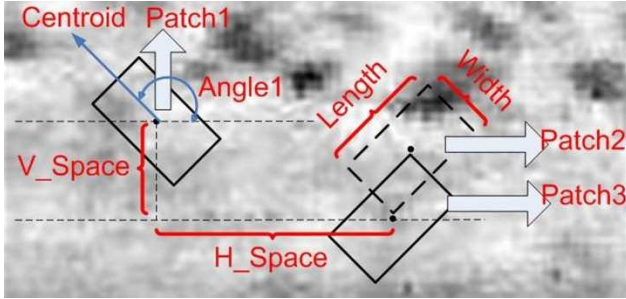


**Figure 2.** Diagram showing some parameters of the proposed iris coding method.

The ‘patch’ is the basic fragment used in our method. To obtain optimum performance we tune the length, width, orientation (angle) and the relative position of a series of patches.

### 3.2 Patch Coding

The procedure for coding a patch is shown in Figure 3. First a 1D intensity signal is obtained by averaging the patch across its width to reduce noise. Using broad patches also makes iris image registration easier, which is important for rotation invariant iris recognition. The FFT is then applied to this 1D signal to obtain spectral coefficients. In order to reduce the spectral leakage during the FFT, a window is employed before the FFT. The Frequency Magnitude Differences between adjacent patches are calculated and a short binary code is generated from the zero crossings of each difference. These constitute the feature vectors of our iris code.

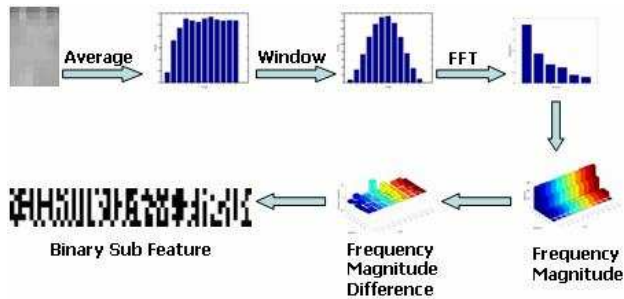


**Figure 3.** Procedure of Patch Coding

### 3.3 Classifier Design

A nearest neighbor classifier is used in matching. The distance between different iris feature vectors is measured by the weighted Hamming Distance, which can be defined as follows:

$$Dis = \frac{1}{A} \sum_{i=1}^N \alpha_i \left[ \frac{1}{B} \sum_{j=1}^M [\beta_j Feature1_{(i,j)} \oplus \beta_j Feature2_{(i,j)}] \right]$$

Here,  $\alpha_i$  denotes the weighting coefficient of different patches, with those nearer the pupil weighted more heavily.  $\beta_j$  is a weight applied to different frequencies, with mid frequencies emphasized.

In order to make the iris recognition system rotation invariant, we code every registered iris image from several initial positions around the circumference. We make seven ‘slip’ templates are made from one registered iris image. An iris to be recognized will be matched to each slip template of the registered iris image and the minimum distance taken as the matching distance.

### 3.4 Experiment Description

The iris database we use to test the performance comes from the CASIA iris database [6]. It has 308 classes of irises and 2174 images (i.e. multiple images of 308 eyes). For each class of iris, three images are selected arbitrarily as a training set, and the others used for testing.

The performance will be tested in two modes: (1) Recognition Mode, in which the CRR (Correct Recognition Rate) is measured, (2) Verification Mode, where the corresponding FAR (False Acceptance Rate) and FRR (False Rejection Rate) will be recorded.

In the next section, we describe the tuning of the parameters used in the method for optimum performance, using two metrics to evaluate the performance: (1) CRR and (2) FAR at first False Rejection.

## 4. FINDING THE OPTIMUM PARAMETERS

### 4.1 Patch Width and Length

Table 1 shows the CRR achieved with different length and width parameters with vertical patches and no windowing. Figure 4 shows the effect of different patch lengths and widths on the FAR at First False Rejection in Verification Mode. We can see that when (Width, Length) equals (8, 12), the system performance is the best both for maximum CRR and minimum FAR. This is chosen as the fundamental patch for the exploration of other parameters.

Length \ Width	8	12	16	24
4	95.20	96.48	96.40	93.92
8	96.96	96.88	96.88	96.16
16	92.40	92.16	89.12	85.28
32	79.20	75.04	70.08	57.60

**Table 1.** CRR (%) tuned by Patch Width and Length

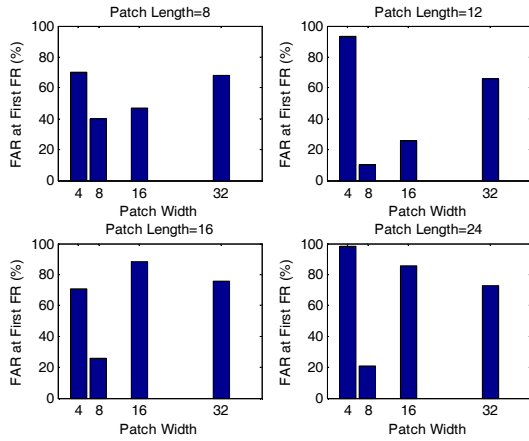


**Figure 4.** Effect of Patch Length and Width on FAR at First False Rejection

#### 4.2 Patch Spacing

The feature vectors are formed from differences between patches. The number of feature vectors possible depends on the spacing of the patches. If the spacing is close or overlapping, many feature vectors will be obtained but they may be similar, so their codes will not be well distributed. If they are too far apart, insufficient vectors may be obtained.

V Space	2	4	6
CRR(%)	99.04	99.92	99.92
V Space	8	10	12
CRR(%)	99.20	98.96	96.88

**Table 2.** CRR (%) tuned by Patch Space

In Table 2, it is seen that the selection of Vertical Spacing is 6 for best CRR, at which patches overlap.

#### 4.3 FFT Window

In order to reduce FFT aliasing, a number of partial Hanning windows were applied to the ends of the data prior to the FFT. In Table 3, it is seen that the best window affects 2 pixels at each end of the data.

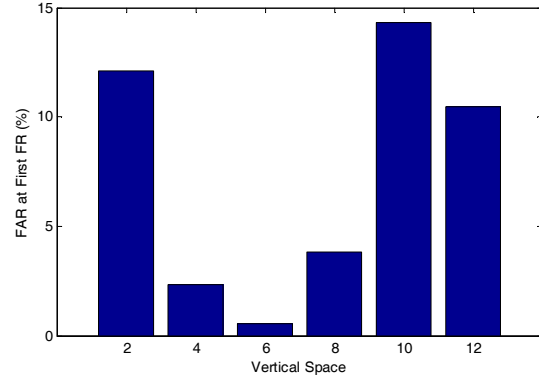


**Figure 5.** Effect of Patch Space on FAR at First False Rejection

Pixels Tapered	6	4	3	2
CRR(%)	96.96	99.60	99.84	99.92
FAR at First False Rejection (%)	26.47	3.24	0.39	0.29

**Table 3.** Performance tuned by Truncated Window.

#### 4.4 Patch Angle

Both Daugman [4] and Tan [6] apply their transforms circumferentially. We have investigated the use of circumferential, radial and diagonal patches. At the 512x48 resolution used, a diagonal patch gives better performance than either circumferential or radial. This is shown by Table 4, in which we achieve 100% CRR. The FAR at First Rejection is also best for the diagonal patch.

Angle	0	45	90
CRR (%)	99.92	100.00	92.40
FAR at First False Rejection (%)	0.2889	0.0039	46.6510

**Table 4.** Performance tuned by Patch Angle

### 5. PERFORMANCE EVALUATION

To assess our method, we apply it to the CASIA database. From each of the 308 classes, we choose arbitrarily 3 images for registration in the database, and test the others for both Recognition (one to many) and Verification (one to one). The parameters we have selected are:

Patch Width=8, Length=12, Angle=45, Window=2, V\_Space=12 and Slip=7, which give 100% CRR.

In Verification Mode, we consider the ROC (Receiver Operating Characteristic) curve which shows the FRR (False Rejection Rate) as a function of FAR (False Acceptance Rate). The FAR is the probability of accepting an imposter and the FRR is the probability of rejecting an authorized person. In the ideal case, the FRR never departs from the FAR axis, meaning that no matter how many imposters are accepted, there is no false rejection, because all the feature vectors of the same class are in one point in the feature space.

Figure 6 compares the ROC of the three algorithms tested in this work on the CASIA database organized as described above.

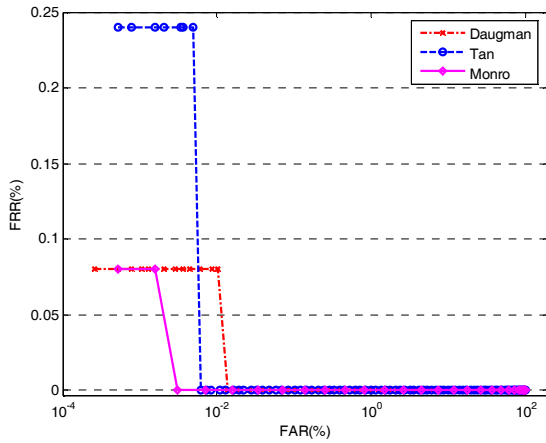


**Figure 6.** Comparison of ROC Curves

In many applications an acceptable FAR would be 0.00003. For example in cash point machines (ATMs) using a four digit PIN, the FAR would be no better than .0001 (assuming that PIN numbers and guesses are random which is probably not the case.) Table 6 is a comparison of FRR when FAR=0.00003.

Method	FRR (%)
Daugman	0.08
Tan	0.25
Monro	0.00

**Table 6.** Comparison at FAR=0.00003

## 6. COMPLEXITY

Complexity is a very important factor in practical applications of iris recognition methods, especially for systems with large databases and real time queries. In Table 7 the speed of the three methods is compared in our MATLAB implementations.

Item \ Method	Feature Extraction (ms)	Match (ms)	Feature Extraction + Match (ms)
Daugman	422	31	453
Tan	125	68	193
Monro	89	31	120

**Table 7.** Comparison of Speed

## 7. DISCUSSION AND CONCLUSIONS

We have developed and evaluated a novel, low complexity coding method for human iris recognition and verification which gives superior performance to the algorithms of Daugman [4] and Tan [6], on the CASIA database, while being of lower complexity. This is *prima facie* an important development. The single failure in the ROC in our experiments is at a FAR of  $2 \times 10^{-3}$  %. Modelling it using a binomial distribution it can be said with 90% confidence that the failure rate lies between  $1.04 \times 10^{-3}$  % and  $3.76 \times 10^{-3}$  %. To narrow this range of uncertainty, evaluation on much larger data sets is required.

## 8. ACKNOWLEDGEMENT

The authors acknowledge the support and sponsorship of Smart Sensors Limited, PO Box 2563, Bath, BA1 3YR, United Kingdom in the development of this new iris coding technique. We are also grateful to Professor T. Tan of the Chinese Academy of Sciences Institute of Automation (CASIA) for use of the CASIA Iris Image Database on which our results are based.

## 9. REFERENCES

- [1] A. Jain, R.M. Bolle and S. Pankanti, Eds., *Biometrics: Personal Identification in a Networked Society*, Norwell, MA: Kluwer, 1999.
- [2] A. Jain, A. Ross and S. Prabhakar, "An Introduction to Biometric Recognition", *IEEE Trans. on Circuits and Systems for Video Technology, Special Issue on Image- and Video-Based Biometrics*, Vol. 14, No. 1, PP. 4-20, January 2004.
- [3] J. Daugman, "Biometric Personal Identification System Based on Iris Analysis", *U.S. Patent*, no. 5291560, 1994
- [4] J. Daugman, "High Confidence Visual Recognition of Persons by a Test of Statistical Independence," *IEEE Trans. on Pattern Analysis and Machine Intelligence*, Vol. 15, No. 11, PP. 1148-1161, 1993
- [5] R. Wildes, etc, " A Machine-vision System for Iris Recognition", *Machine Vision and Applications*, Vol. 9, PP. 1-8, 1996
- [6] L. Ma, T. Tan, etc, "Efficient Iris Recognition by Characterizing Key Local Variations," *IEEE Trans. on Image Processing*, Vol. 13, PP. 739-750, 2004.